The nuclear localization signal is required for the function of *squamosa promoter binding protein-like gene 9* to promote vegetative phase change in *Arabidopsis*

Hui Zhang[1] · Lu Zhang[1] · Junyou Han[2] · Zhiyuan Qian[1] · Bingying Zhou[1] · Yunmin Xu[1] · Gang Wu[1]

Abstract

Key message **A mutation in the nuclear localization signal of** *squamosa promoter binding like-protein 9(SPL9)* **delays vegetative phase change by disrupting its nuclear localization.**

Abstract The juvenile-to-adult phase transition is a critical developmental process in plant development, and it is regulated by a decrease in miR156/157 and a corresponding increase in their targets, *squamosa promoter binding protein-like* (*SPL*) *genes*. SPL proteins contain a conserved SBP domain with putative nuclear localization signals (NLSs) at their C-terminals. Some SPLs promote vegetative phase change by promoting miR172 expression, but the function of nuclear localization signals in those SPLs remains unknown. Here, we identified a loss-of-function mutant, which we named *del6*, with delayed vegetative phase change phenotypes in a forward genetic screen. Map-based cloning, the whole genome resequencing, and allelic complementation test demonstrate that a G-to-A substitution in the *SPL9* gene is responsible for the delayed vegetative phase change phenotypes. In *del6*, the mutation causes a substitution of the glutamine (Gln) for the conserved basic amino acid arginine (Arg) in the NLS of the SBP domain, and disrupts the normal nuclear localization and function of SPL9. Therefore, our work demonstrates that the NLSs in the SBP domain of SPL9 are indispensable for its nuclear localization and normal function in *Arabidopsis*.

Keywords Vegetative phase change · SPL9 · SBP domain · Nuclear localization signals (NLS)

Hui Zhang, Lu Zhang and Junyou Han have contributed equally to this work.

Electronic supplementary material The online version of this article (https://doi.org/10.1007/s11103-019-00863-5) contains supplementary material, which is available to authorized users.

✉ Yunmin Xu
xuyunmin@zafu.edu.cn

✉ Gang Wu
wugang@zafu.edu.cn

1 State Key Laboratory of Subtropical Silviculture, Laboratory of Plant Molecular and Developmental Biology, Zhejiang Agriculture and Forestry University, Hangzhou, China

2 College of Plant Science, Jilin University, Changchun 130062, China

Introduction

After germination, the plant shoot apex passes through two different phases: a vegetative phase and a reproductive phase. The vegetative phase could be further divided into a juvenile vegetative phase and an adult vegetative phase. In addition to their difference in reproductive competence, the juvenile and adult vegetative phases can also be distinguished by a series of distinct phase-specific traits including morphological, physiological, and biochemical traits (Poethig 2003, 2013). The transition from the juvenile to the adult vegetative phase is referred to as vegetative phase change. In *Arabidopsis*, vegetative phase change is marked by an increase in the degree of serration of the leaf margin, an increase in the leaf length/width (L/W) ratio, a decrease in cell size, and the production of trichomes on the abaxial side of leaf blades (Poethig 1990; Telfer et al. 1997).

Vegetative phase change in plants is regulated by a decrease in the level of miR156/157 and a corresponding increase in their targets, the *SPL* genes (Wu and Poethig

2006; Wu et al. 2009a, b). SBPs (*SQUAMOSA* promoter binding proteins, SBPs) were originally identified in *Antirrhinum majus* as factors that bind to the promoter of the floral meristem identity gene *SQUAMOSA* (Klein et al. 1996). Later, they were identified in all green plants, and they constitute a plant-specific transcription factor family (Guo et al. 2008). Except for the conserved SBP domain with ~ 75 amino acids, plant SPLs are diverse in their primary structures. Nuclear magnetic resonance (NMR) results showed two, non-interleaved Zn^{2+} coordinating structures within SBP domains, and they are formed by eight conserved cysteine and histidine residues (Yamasaki et al. 2004). Amino acid exchange experiments indicate that each Zn^{2+} structure is essential for the binding to the GTAC core motif (Birkenbihl et al. 2005).

The Arabidopsis genome encodes 17 *SPL* genes, and 10 *SPL* genes including *SPL2*, *SPL3*, *SPL4*, *SPL5*, *SPL6*, *SPL9*, *SPL10*, *SPL11*, *SPL13*, and *SPL15* are shown to be repressed by miR156 by transcript cleavage or translational inhibition (He et al. 2018). Based on their functional diversity, miR156-targeted genes can be categorized into 3 functionally different groups. *SPL9*, *SPL13*, *SPL15*, *SPL2*, *SPL10* and *SPL11* function to promote vegetative phase change with *SPL9*, *SPL13* and *SPL15* playing much more important roles than others; *SPL6* functions in certain physiological processes, and *SPL3*, *SPL4*, *SPL5* function to regulate floral meristem identity (Xu et al. 2016).

It has been shown that nuclear import of transcription factors is essential for their function, it is usually initiated by the binding of importin α to NLS (Görlich and Kutay 1999; Kaffman and O'Shea 1999; Jans et al. 2000). A putative bipartite NLS overlapping with the second Zn^{2+} motif was identified at the C terminal of the SBP domain, characterized by two basic amino acid clusters spaced by 11 amino acid residues (Stone et al. 2005; Birkenbihl et al. 2005). This putative bipartite NLS is required for the nuclear import of SPL3 and SPL8, and a truncation of the complete second part of the bipartite NLS of SPL3 decreased the nuclear import of SPL3 (Birkenbihl et al. 2005). Although this putative bipartite NLS is conserved in all SPLs, the nuclear import efficiency is different among different SPLs, implying that some additional basic regions may function as NLS (Birkenbihl et al. 2005). How different putative NLSs in SPLs affect nuclear import and therefore their functions in plant development and growth remains unclear.

In this study, we identified a loss-of-function mutant with delayed vegetative phase change phenotypes in a forward genetic screen, which we named *delayed juvenile-to-adult phase transition mutant 6* (*del6*). Map-based cloning, the whole genome re-sequencing, and genetic analysis indicate that the Arginine-to-glutamine substitution at the conserved SBP domain of SPL9 is responsible for the phenotype. This mutation disrupted the conserved NLS of SPL9, and caused abnormal nuclear localization pattern of SPL9 in the plant cell, thus abolishing the normal function of SPL9 in vegetative phase change. Our work here therefore demonstrated that the NLS at the C-terminus of SBP is critical for SPL9 normal nuclear localization and function in vegetative phase change.

Materials and methods

Genetic stocks and growth conditions

Genetic stocks used in this study were all in the Columbia (Col) genetic background. *spl9-4* (SAIL_150_B05, a null allele mutant) was obtained from the Arabidopsis Biological Resource Center (Columbus, OH, United States). Seeds were sown in a moistened 1:1 mixture of soil:vermiculite and left at 4 °C for 48 h before being transferred to the growth chamber. Plants were grown in short day (SD, 10-h light, 14-h darkness, 140 μm/m^2/s, 22 °C). Plant age was measured from the time when seeds were transferred to the growth chamber. Abaxial trichomes were scored 2–3 weeks after planting with a stereomicroscope. For leaf shape analysis, fully expanded leaves were removed, attached to cardboard with double-sided tape and flattened with transparent tape, and then scanned in a digital scanner.

Map-based cloning and whole genome re-sequencing

To map the *DEL6* locus, the *del6* (Col background) mutant was crossed to Landsberg *erecta* (Ler), and the selfed F2 individuals exhibiting the *del6* phenotype, including rounder leaves with fewer serrations and abaxial trichomes later than leaf fourteen were chosen for mapping. For the whole genome re-sequencing, the *del6* mutant was backcrossed to Col plants, and sixty different F2 individuals with the *del6* phenotype were chosen to take leaf samples, and DNA from the mixed leaf samples was sent for the whole genome re-sequencing. Based on the above mapping and the whole genome re-sequencing data, we searched for G-to-A and/or C-to-T mutations in the candidate region to pin down the mutation responsible for the *del6* phenotype.

NLS and phosphorylation site prediction

The putative NLSs in different SPLs were predicted using the PSORTII program (http://psort.hgc.jp). The potential phosphorylation sites were predicted using the NetPhos 3.1 Server (http://www.cbs.dtu.dk/services/NetPhos/).

Vector construction and plant transformation

35S::GFP plasmid is a lab stock. The CDS sequence of *SPL9* was amplified using cDNA samples from both WT and *del6*, and then were fused to GFP under the control of the *35S* promoter to generate *35S::GFP-SPL9^{WT}* and *35S::GFP-SPL9^{del6}* plasmids, respectively. Transient expression and subcellular localization analysis of GFP-fused proteins were done following a previous study (Wu et al. 2009). About a five-kb genomic fragment of *SPL9* from both WT and *del6* mutant were amplified and cloned into *pCAMBIA1305.1* to generate *gSPL9^{WT}* and *gSPL9^{del6}* expression vectors. These two expression vectors were then transformed into *Agrobacterium tumefaciens* strain GV3101 to transform Arabidopsis using the floral dipping method. Seeds of transformed plants were collected and sown on half strength MS medium containing hygromycin (50 mg/L) to select for transgenic plants. Eight independent homozygous transgenic lines (*gSPL9^{WT}* 1-8 lines, *gSPL9^{del6}* 1-8 lines) were selected randomly for further characterization in this study.

Results

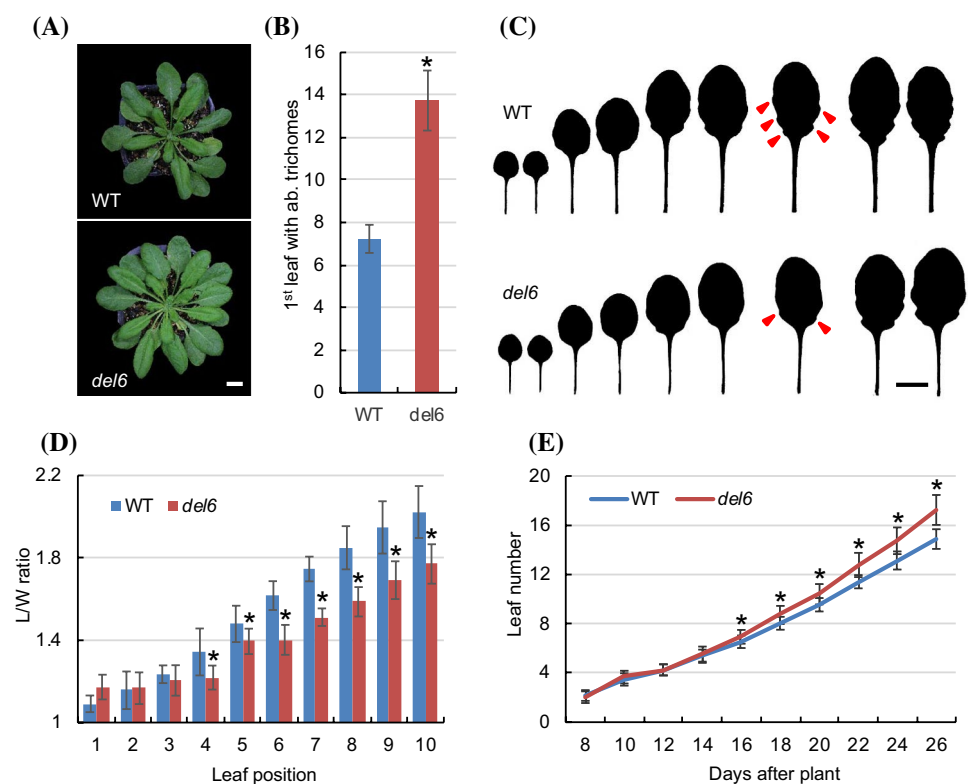### The *del6* mutant delays vegetative phase change

We identified a mutant with delayed vegetative phase change phenotypes in a forward genetic screen of an ethylmethanesulfonate (EMS)-mutagenized M2 population (Fig. 1a). In short day, wild type produced abaxial trichomes on leaf 7.23 ± 0.66, the *del6* mutant had abaxial trichomes on leaf 13.73 ± 1.41, which was significantly later than wild type (Fig. 1b). Measurement of leaf length to width ratio (L/W ratio) showed that the *del6* mutant had significantly smaller ratio than wild type, suggesting that leaves from the *del6* mutant were much rounder than those from wild type, especially for those after the third leaf (Fig. 1c, d). The late-formed leaves from *del6* also had fewer serrations than their counterparts from wild type (Fig. 1c). In addition, the *del6* mutant had significantly faster leaf initiation rate than wild type (Fig. 1a, e). These results indicate the *del6* mutant exhibits typical delayed vegetative phase change phenotypes.

Map-based cloning of *DEL6*

To map the *del6* mutation, the *del6* mutant was first crossed to Landsberg *erecta*, and the selfed F2 individuals with the *del6* phenotype were selected for map-based cloning. The mutation was narrowed down to a ca.3200 Kb region on chromosome 2 between position 16291 K and 19542 K) (Fig. S1). Next, we used the whole genome re-sequencing method to identify mutations in this region. The sequencing result indicated that there were six different mutations within this candidate region, and one of them is located within the *SPL9* coding region (Fig. S2). SPL9 has been shown to promote vegetative phase change, and loss-of-function mutation

Fig. 1 *del6* delays vegetative phase change in *Arabidopsis*. **a** 5-week-old plants grown in short day (SD). Scale: 1 cm. **b** The first leaf with abaxial trichomes in wild type (WT) and *del6* in SD. The asterisks denote the significant difference from WT at $P < 0.01$ using Student's *t*-test (Data are mean ± SD from n = 37 plants). **c** Leaf shape of WT and *del6* in SD. Red triangles indicate leaf serrations on the 6th leaf margin. Scale: 1 cm. **d** Leaf length/width (L/W) ratio of different leaves from WT and *del6* in SD. Asterisks denote the significant difference from WT at $P < 0.01$ using Student's *t*-test (Data are mean ± SD from n = 37 plants). **e** Leaf initiation rate of WT and *del6* in SD. Asterisks denote the significant difference from WT at $P < 0.01$ (Data are mean ± SD from n = 37 plants)

of *SPL9* delays vegetative phase change (Wu et al. 2009a, b; Xu et al. 2016). Therefore, we proposed that the mutation in the SPL9 coding region might be responsible for the *del6* mutant phenotype. Based on the availability of different *spl9* alleles (four T-DNA insertional mutant alleles, *spl9-1* to *spl9-4*) (Schwarz et al. 2008; Xu et al. 2016), we renamed the *del6* mutant as *spl9-5*. In *spl9-5* (*del6*), there is a G-to-A substitution at the +434 bp from the start codon in the *SPL9* sequence (Fig. S3), this causes a replacement of 145-Arg by a Gln within the SBP conserved domain (Fig. 2a).

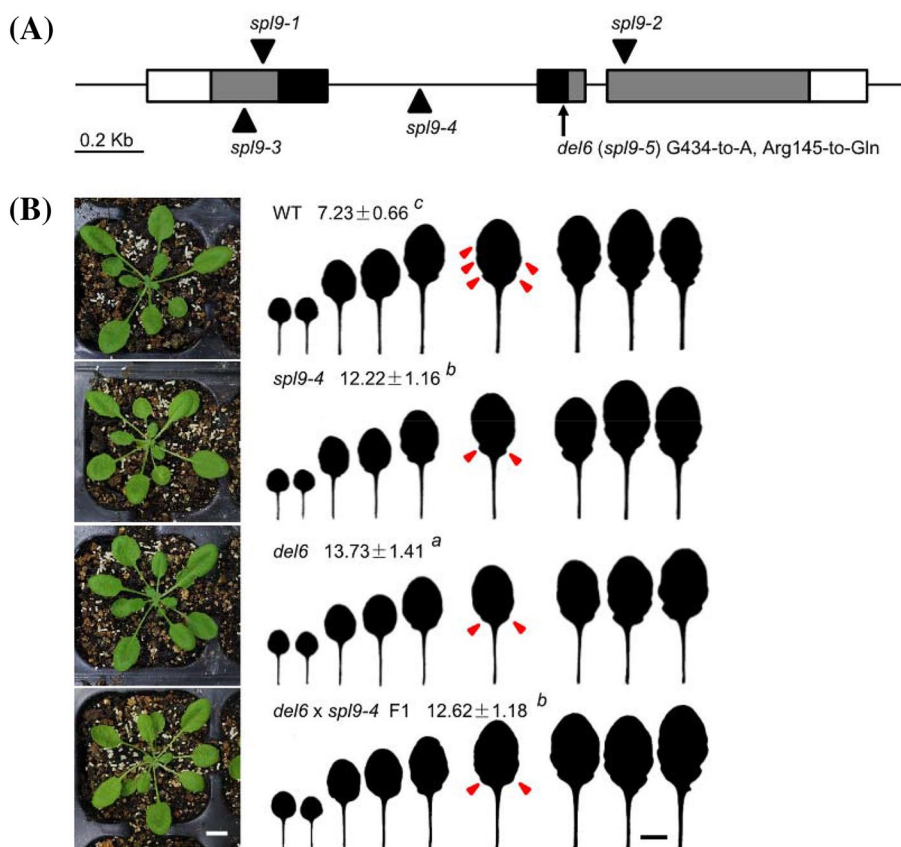### *del6* acts as a new allelic mutant of the *SPL9* gene

To further conform that the mutation in the *SPL9* gene is responsible for the *del6* mutant phenotype, we did a genetic complementation test by crossing *del6* to *spl9-4*. In short day, *del6* and *spl9-4* produced abaxial trichomes on leaf 13.73 ± 1.41 and 12.22 ± 1.16, respectively; whereas wild type produced abaxial trichomes on leaf 7.23 ± 0.66, which was significantly earlier than *del6* and *spl9-4*, and *del6* and *spl9-4* also lacked serrations on leaf margin compared with wild type (Fig. 2b). The F1 progeny plants from the cross between *del6* and *spl9-4* had almost similar abaxial trichome production to *spl9-4* (Fig. 2b), this indicates that *del6* was unable to complement the *spl9-4* phenotype, suggesting that *del6* and *spl9-4* are allelic. This result demonstrates that the

del6 mutant phenotype is truly attributable to the mutation in the *SPL9* gene.

del6 has a mutation in the conserved putative NLSs

Previous studies have shown that there is a putative bipartite NLS within the SBP domain at the C terminals of SPL proteins (Fig. 3a), and it overlaps with the second Zn-coordinating structure (Zn-2 motif) (Stone et al. 2005; Birkenbihl et al. 2005). In this study, we identified three putative NLSs in SPL9 using the POSRTII program. These include a monopartite NLS 1 between amino acid aa-71 and aa-74 in a context of RRRK, a monopartite NLS 2 between aa-72 and aa-75 in a context of RRKP, and a bipartite NLS 1 between aa-58 and aa-74 in a context of KRSCRRRLAGHNERRRK (Fig. 3b). These NLS are located at the C-terminal of the SBP domain, and the bipartite NLS 1 was also described by previous studies (Stone et al. 2005; Birkenbihl et al. 2005) and characterized by clusters with two basic amino acids separated by 11 amino acids. In *del6*, the mutation is located in the conserved putative bipartite NLS (Fig. 3a, b), resulting in the replacement of the conserved basic amino acid arginine at aa-72 by a glutamine (Fig. 3b). This putative bipartite NLS was shown to be required for the nuclear import of SPL3 and SPL8 (Birkenbihl et al. 2005), but how

Fig. 2 A mutation in the *SPL9* gene is responsible for the delayed vegetative phase change phenotype in *del6*. **a** Available loss-of-function mutant alleles for *SPL9*. *del6* contains a G-to-A substitution in the *SPL9* gene. *spl9-1 ~ spl9-4* are T-DNA insertional mutants. The white box indicates noncoding region, the light black box indicates coding region, and the dark black indicates SBP box. **b** The genetic complementation test result for *del6* and *spl9-4*. Leaf shape and the first leaf with abaxial trichomes in 3-week-old WT, *del6*, *spl9-4*, and F1 plants from a cross between *del6* and *spl9-4* in SD. Different letters indicate significant difference between genotypes using one-way ANOVA at $P < 0.01$ (Data are mean $\pm$ SD from n = 37 plants). Leaf serration on the 6th leaf blade is marked with red triangles. Scale bar: 1 cm

(A)

Zn-1   Zn-2

(B)

Monopartite NLS 1 (aa 71-74)
Monopartite NLS 2 (aa 72-75)
Bipartite NLS 1 (aa 58-59 and aa 71-74)
Bipartite NLS 2 (aa 62-64 and aa 71-74)

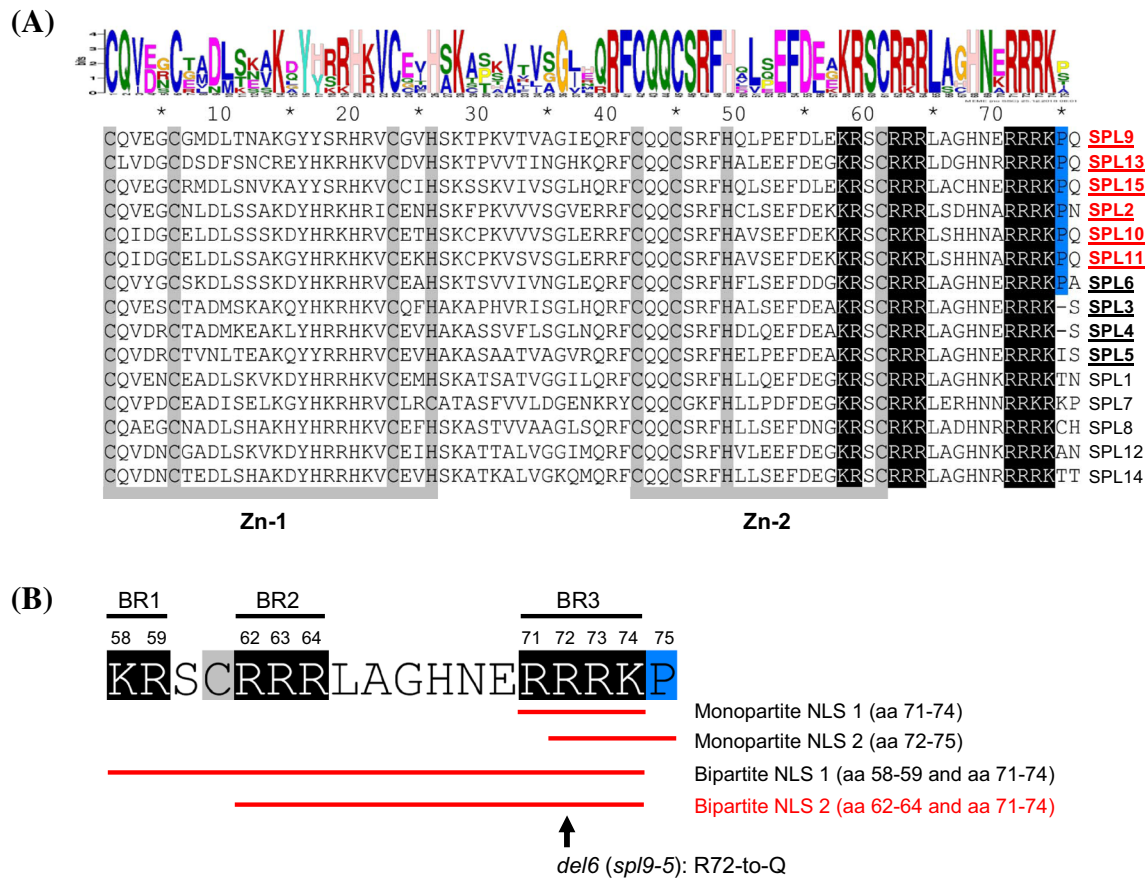*del6* (*spl9-5*): R72-to-Q

Fig. 3 *del6* disrupts a putative conserved nuclear localization signal in SPL9. **a** Cluster analysis of the SBP domain of different SPL proteins using MEME. The two Zn-coordinating structures (Zn-1 and Zn-2) are highlighted with grey according to previous studies (Yamasaki et al. 2004; Birkenbihl et al. 2005). The conserved basic amino acid clusters are highlighted with black, the conserved proline within Group I SPLs is highlighted with blue. Numbers indicate the relative amino acid position in the conserved SBP domain. **b** Three basic amino acid clusters (BR1~3) and the fourth putative NLSs at the C terminal of SBP domain. Monopartite NLS 1, monopartite NLS 2 and bipartite NLS 1 are predicted using the POSRTII program, bipartite NLS 2 is predicted according to a previous study (Zhu et al. 2015). R72-to-Q mutation in *del6* (*spl9-5*) is marked with an arrow. Numbers indicate the relative amino acid position in the conserved SBP domain

this mutation in *del6* affects SPL9 nuclear import therefore its function remains unknown.

Mutation in the NLS in SBP domain of SPL9 changes the nuclear localization of SPL9

Since the mutation in *del6* is located in the conserved putative NLS, we hypothesized that the phenotype of *del6* might be attributable to its defects in nuclear localization. Therefore, we studied the nuclear localization of SPL9 and DEL6 using Arabidopsis mesophyll protoplast transformed with *35S::GFP*, *35S::GFP-SPL9^{WT}* (*SPL9* CDS from WT), and *35S::GFP-SPL9^{del6}* (*SPL9* CDS from the *del6* mutant) plasmids, respectively. In the transient expression assay with *35S::GFP*, the GFP signal was mainly concentrated in the nucleus, as well as some distribution of GFP signals in the cytoplasm (Fig. 4). In the assay with *35S::GFP-SPL9^{WT}*,

GFP was specifically localized in the nucleus, implying that the GFP-SPL9^{WT} protein was imported efficiently into the nucleus. In contrast, the GFP-SPL9^{del6} fusion protein was diffusible in the plant cell, and a large proportion of the GFP signal was retained in the cytoplasm in addition to its nuclear distribution (Fig. 4). This result suggests that the *del6* mutation changes the specific nuclear localization of SPL9, and the conserved NLS in the SBP domain is indispensable for the correct nuclear localization of SPL9 in the plant cell.

The NLS is required for the function of SPL9 in plants

To future conform if the conserved NLS is required for the function of SPL9, we amplified the genomic sequence of *SPL9* from wild type and *del6*, and cloned them into the *pCAMBIA1305.1* expression vector, and transformed

Fig. 4 Subcellular localization of eGFP, eGFP-SPL9^{WT} and eGFP-SPL9^{del6} fusion proteins. Plasmids were delivered to protoplast using the PEG-mediated method. After 16 h of transformation, GFP distribution in cells were examined with a confocal fluorescent microscopy. Scale: 10 μm
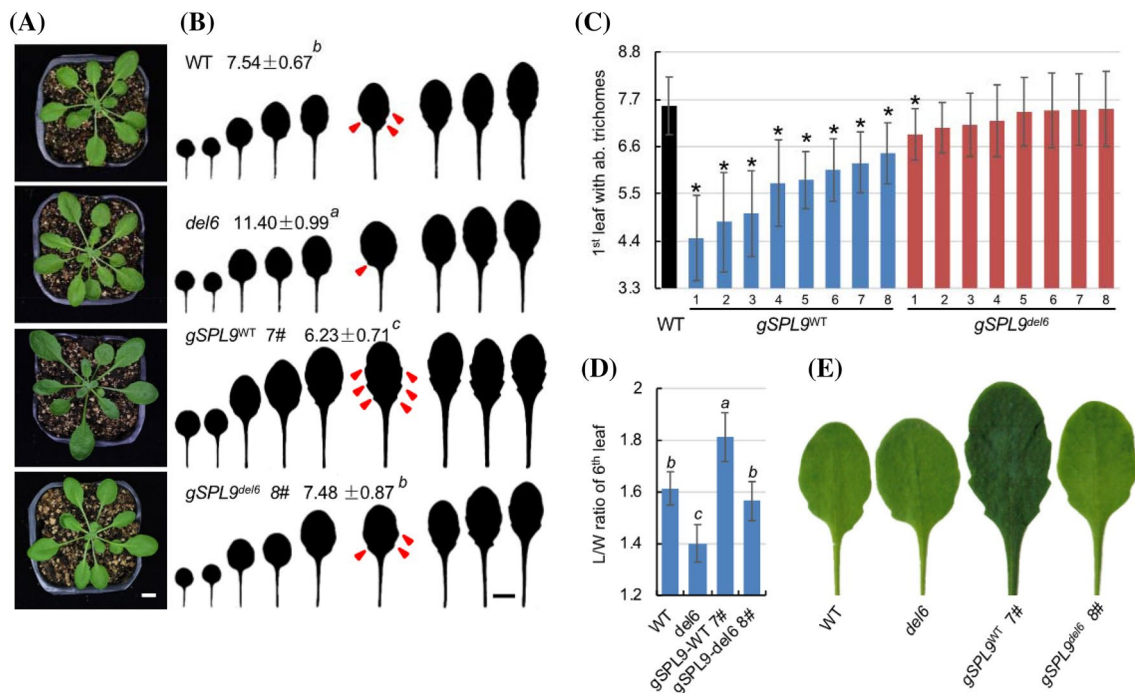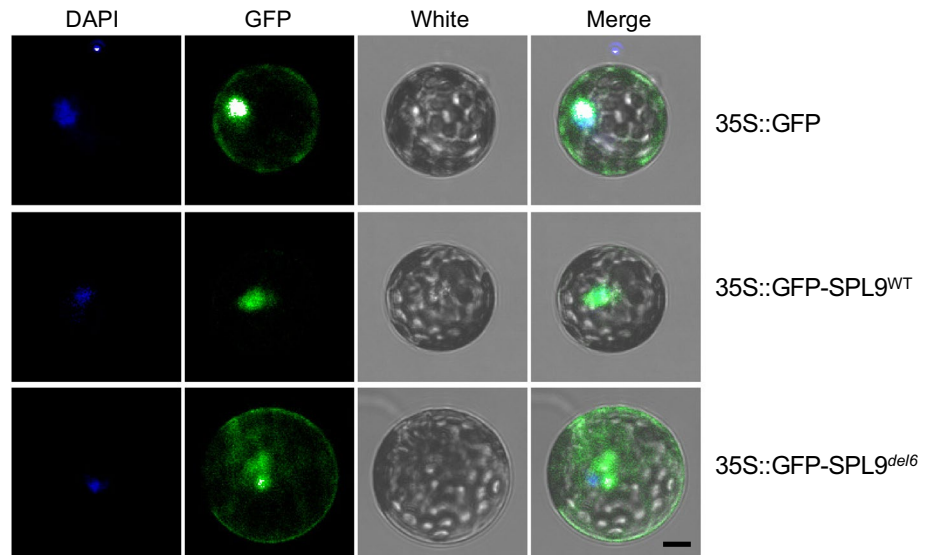
Fig. 5 The G-to-A substitution in SPL9 impairs its function to promote vegetative phase change. **a** 4-week-old WT, *del6*, *gSPL9^{WT}*, and *gSPL9^{del6}* transgenic plants grown in SD. *gSPL9^{WT}*: transgenic plants transformed with the wild-type *SPL9* genomic sequence under the control of its native promoter; *gSPL9^{del6}*: transgenic plants transformed with the *del-6* mutant *SPL9* genomic sequence under the control of its native promoter. Scale: 1 cm. **b** Leaf shape and the first leaf with abaxial trichomes. Leaf serrations on the 6th leaf margin are marked with red triangles. Different letters indicate significant difference between genotypes using one-way ANOVA at $P < 0.01$ (Data are mean ± SD from n = 17 plants). Scale: 1 cm. **c** The first leaf with abaxial trichomes from WT and different *gSPL9^{WT}* and *gSPL9^{del6}* transgenic lines. Asterisks denote the significant difference from WT at $P < 0.01$ (Data are mean ± SD from n = 17 plants). **d** Leaf L/W ratio of the 6th leaf from different genotypes. Different letters indicate significant difference between genotypes using one-way ANOVA at $P < 0.01$ (Data are mean ± SD from n = 10 individual plant). **e** Leaves from *gSPL9^{WT}* transgenic lines are dark green. The 6th leaf from different genotypes are used. Scale: 1 cm

wild-type Arabidopsis plants to generate $gSPL9^{WT}$ and $gSPL9^{del6}$ transgenic plants, respectively. We randomly chose 8 independent homozygous transgenic lines with single T-DNA insertions from both $gSPL9^{WT}$ and $gSPL9^{del6}$ transgenic plants, and characterized the vegetative phase change phenotype of these plants. In short day, $gSPL9^{WT}$ transgenic plants produced abaxial trichomes significantly earlier than wild type (6.23 ± 0.71 versus 7.54 ± 0.67), whereas $gSPL9^{del6}$ transgenic plants had abaxial trichomes similar to wild type (7.48 ± 0.87 versus 7.54 ± 0.67) (Figs. 5, S4); moreover, leaves of $gSPL9^{WT}$ were significantly elongated and had more serrations on leaf margins than wild type and *del6*, whereas leaves of $gSPL9^{del6}$ were similar to those of wild type (Fig. 5b, d). Leaves of $gSPL9^{WT}$ were also dark green (Fig. 5e). These results demonstrate that the mutation in the NLS of the *SPL9* gene disrupts the normal function of SPL9 in vegetative phase change.

Discussion

SPLs belong to a plant specific transcription factors family with diverse roles in plant growth and development. In *Arabidopsis*, ten different SPLs are targets of miR156, and six of them (Group I) function to promote vegetative phase change (Fig. S5a, b) (Xu et al. 2016). SPL proteins are characterized by a conserved SBP domain at their C-terminals with three putative NLSs. The function of those NLSs has not been elucidated so far. Here, we showed that the NLSs of SPL9 are indispensable for its normal function. These NLSs affect SPL9 function by changing its nuclear localization in the plant cell. Typical NLSs contain one (monopartite) or two (bipartite) clusters of basic residues. Monopartite NLSs, exemplified by SV40 T-antigen, have a single cluster of four or five basic residues (Conti et al. 1998; Conti and Kuriyan 2000), whereas bipartite NLSs, exemplified by *Xenopus laevis* protein nucleoplasmin, have two clusters of basic residues separated by a flexible linker of 9–12 amino acids (Robbins et al. 1991; Dingwall and Laskey 1991; Jans et al. 2000). SPL9 contains a region rich in basic amino acids at the C terminal of the SBP domain (aa58-75 KRSCRRRLAGHNERRRKP), it contains three clusters with basic amino acids designated as BR1(aa58-59 KR), BR2 (aa62-64 RRR) and BR3 (aa71-74 RRRK) in the SBP domain (Fig. 3b). We identified three potential NLSs within this region using PSORT including a monopartite NLS 1 (aa71-74 RRRK) and a monopartite NLS 2 (aa72-75 RRKP) in BR3, and a bipartite NLS 1 (aa58-74 KRSCRRRLAGHNERRRK) consisting of BR1 and BR3 (Fig. 3b). In monopartite NLS 2, there is a conserved proline residue at aa75. Interestingly, this proline is only present in SPL proteins including SPL2, SPL9, SPL10, SPL11, SPL13, and SPL15 shown to play important roles in vegetative phase

change (except for SPL6). Recent studies showed that the flexible linker for the bipartite NLSs can be up to 29 aa in Ty1 integrase (Lange et al. 2010), or to 7 aa in IRF3 (Zhu et al. 2015). This suggests that the traditional way of defining bipartite NLSs is too restrictive, and the linker size can vary depending on amino acid composition or conformation. According to this rule, the sequence of 62-74 RRRLAGHNERRRK in the SBP domain of SPL9 contains BR2 and BR3, and it can also possibly function as a bipartite NLS 2 with a 6 aa linker (Fig. 3b). Obviously, all above NLSs requires the presence of the BR3 region (72-74 RRK), as shown by the *del6* mutation that the R72-to-Q substitution in BR3 completely disrupted the normal function of SPL9. Whether BR3 functions as a monopartite NLS, or together with BR1 or BR2 as a bipartite NLSs, needs further investigation.

Covalent modification of nuclear proteins, especially within and/or adjacent to the NLS, can affect the binding affinity of NLS for importin α, and change the nuclear import efficiency (Harreman et al. 2004; Birkenbihl et al. 2005). We identified two potential phosphorylation sites, Serine at aa60 (S60) and the Serine/Threonine at aa101 (S/T101), adjacent to the NLS in SPL9 and other SPL proteins using NetPhos (Fig. S5b). S60 is located in the conserved SBP domain, and the S/T101 is located ~20 aa downstream of NLS. The biological function of S60 phosphorylation has been investigated in a previous study (Birkenbihl et al. 2005). S60 phosphorylation in SPL3 doesn't affect the nuclear import efficiency, but S60 phosphorylation negatively influences SPL8 nuclear import efficiency. In contrast, S60 phosphorylation in OsSPL14 (the SPL9 homolog in rice) changed its DNA binding activity in that the non-phosphorylated OsSPL14 preferentially binds to the GTAC motif, while the S60-phosphorylated OsSPL14 preferentially binds to the TGGGCC motif without altering its nuclear localization. S60 phosphorylation in OsSPL14 could be induced by fungus infection to balance between growth and immunity (Wang et al. 2018). Among different clades in SPL family, the Group II SPLs including SPL3, SPL4, and SPL5 contains a conserved putative phosphorylation site at S76, and Group I SPLs including SPL2, SPL10, and SPL11 contain a conserved potential phosphorylation site at S66 (Fig. S5a, b). Questions of whether S66, S76 and S/T101 site are subjected to phosphorylation and how this potential modification affects the function of different SPL genes will be an important task to deepen our understanding of how vegetative phase change is regulated in plants.

Author contribution YX and GW conceived and designed the research, HZ, JH, LZ, ZQ and BZ performed the experiments, YX and GW wrote the manuscript.

References

Birkenbihl RP, Jach G, Saedler H, Huijser P (2005) Functional dissection of the plant-specific SBP-Domain: overlap of the DNA-binding and nuclear localization domains. J Mol Biol 352:585–596

Conti E, Kuriyan J (2000) Crystallographic analysis of the specific yet versatile recognition of distinct nuclear localization signals by karyopherin α. Structure 8:329–338

Conti E, Uy M, Leighton L, Blobel G, Kuriyan J (1998) Crystallographic analysis of the recognition of a nuclear localization signal by the nuclear import factor karyopherin α. Cell 94:193–204

Dingwall C, Laskey RA (1991) Nuclear targeting sequences a consensus? Trends Biochem Sci 16:478–481

Görlich D, Kutay U (1999) Transport between the cell nucleus and the cytoplasm. Annu Rev Cell Dev Biol 15:607–660

Guo A, Zhu Q, Gu X, Ge S, Yang J, Luo J (2008) Genome-wide identification and evolutionary analysis of the plant specific SBP-box transcription factor family. Gene 418:1–8

Harreman MT, Kline TM, Milford HG, Harben MB, Hodel AE, Corbett AH (2004) Regulation of nuclear import by phosphorylation adjacent to nuclear localization signals. J Biol Chem 279:20613–20621

He J, Xu M, Willmann MR, McCormick K, Hu T, Yang L, Starker CG, Voytas DF, Meyers BC, Poethig RS (2018) Threshold-dependent repression of SPL gene expression by miR156/miR157 controls vegetative phase change in *Arabidopsis thaliana*. PLoS Genet 14:e1007337

Jans DA, Xiao CY, Lam MH (2000) Nuclear targeting signal recognition: a key control point in nuclear transport? BioEssays 22:532–544

Kaffman A, O'Shea EK (1999) Regulation of nuclear localization: a key to a door. Annu Rev Cell Dev Biol 15:291–339

Klein J, Saedler H, Huijser P (1996) A new family of DNA binding proteins includes putative transcriptional regulators of the *Antirrhinum majus* floral meristem identity gene SQUAMOSA. Mol Gen Genet 250:7–16

Lange A, McLane LM, Mills RE, Devine SE, Corbett AH (2010) Expanding the definition of the classical bipartite nuclear localization signal. Traffic 11:311–323

Poethig RS (1990) Phase change and the regulation of shoot morphogenesis in plants. Science 250:923–930

Poethig RS (2003) Phase change and the regulation of developmental timing in plants. Science 301:334–336

Poethig RS (2013) Vegetative phase change and shoot maturation in plants. Curr Top Dev Biol 105:125–152

Robbins J, Dilworth SM, Laskey RA, Dingwall C (1991) Two interdependent basic domains in nucleoplasmin nuclear targeting sequence: identification of a class of bipartite nuclear targeting sequence. Cell 64:615–623

Schwarz S, Grande AV, Bujdoso N, Saedler H, Huijser P (2008) The microRNA regulated SBP-box genes SPL9 and SPL15 control shoot maturation in Arabidopsis. Plant Mol Biol 67:183–195

Stone JM, Liang X, Nekl ER, Stiers JJ (2005) Arabidopsis AtSPL14, a plant-specific SBP-domain transcription factor, participates in plant development and sensitivity to fumonisin B1. Plant J 41:744–754

Telfer A, Bollman KM, Poethig RS (1997) Phase change and the regulation of trichome distribution in *Arabidopsis thaliana*. Development 124:645–654

Wang J, Zhou L, Shi H, Chern M, Yu H, Yi H, He M, Yin J, Zhu X, Li Y, Li W, Liu J, Wang J, Chen X, Qing H, Wang Y, Liu G, Wang W, Li P, Wu X, Zhu L, Zhou J, Ronald P, Li S, Li J, Chen X (2018) A single transcription factor promotes both yield and immunity in rice. Science 361:1026–1028

Wu G, Poethig RS (2006) Temporal regulation of shoot development in Arabidopsis thaliana by miR156 and its target SPL3. Development 133:3539–3547

Wu F, Shen S, Lee L, Lee S, Chan M, Lin C (2009a) Tape-Arabidopsis Sandwich-a simpler Arabidopsis protoplast isolation method. Plant Methods 5:16

Wu G, Park M, Conway SR, Wang JW, Weigel D, Poethig RS (2009b) The sequential action of miR156 and miR172 regulates developmental timing in Arabidopsis. Cell 138:750–759

Xu M, Hu T, Zhao J, Park M, Earley KW, Wu G, Yang L, Poethig RS (2016) Developmental functions of miR156-regulated squamosa promoter binding protein-likE (SPL) genes in *Arabidopsis thaliana*. PLoS Genet 12:e1006263

Yamasaki K, Kigawa T, Inoue M, Tateno M, Yamasaki T, Yabuki T, Aoki M, Seki E, Matsuda T, Nunokawa E, Ishizuka Y, Terada T, Shirouzu M, Osanai T, Tanaka A, Seki M, Shinozaki K, Yokoyama S (2004) A novel zinc-binding motif revealed by solution structures of DNA-binding domains of arabidopsis SBP-family transcription factors. J Mol Biol 337:49–63

Zhu M, Fang T, Li S, Meng K, Guo D (2015) Bipartite nuclear localization signal controls nuclear import and DNA-binding activity of IFN regulatory factor 3. J Immunol 195:289–297

Publisher's Note Springer Nature remains neutral with regard to jurisdictional claims in published maps and institutional affiliations.